Molecular Cancer Therapeutics

Mechanisms of Acquired Resistance to Trastuzumab Emtansine in Breast Cancer Cells

Guangmin Li[1], Jun Guo[1], Ben-Quan Shen[2], Daniela Bumbaca Yadav[2], Mark X. Sliwkowski[1], Lisa M. Crocker[1], Jennifer A. Lacap[1], and Gail D. Lewis Phillips[1]

Abstract

The receptor tyrosine kinase HER2 is overexpressed in approximately 20% of breast cancer, and its amplification is associated with reduced survival. Trastuzumab emtansine (Kadcyla, T-DM1), an antibody–drug conjugate that is comprised of trastuzumab covalently linked to the antimitotic agent DM1 through a stable linker, was designed to selectively deliver DM1 to HER2-overexpressing tumor cells. T-DM1 is approved for the treatment of patients with HER2-positive metastatic breast cancer following progression on trastuzumab and a taxane. Despite the improvement in clinical outcome, many patients who initially respond to T-DM1 treatment eventually develop progressive disease. The mechanisms that contribute to T-DM1 resistance are not fully understood. To this end, we developed T-DM1–resistant *in vitro* models to examine the mechanisms of acquired T-DM1 resistance. We demonstrate that decreased HER2 and upregulation of MDR1 contribute to T-DM1 resistance in KPL-4 T-DM1–resistant cells. In contrast, both loss of SLC46A3 and PTEN deficiency play a role in conferring resistance in BT-474M1 T-DM1–resistant cells. Our data suggest that these two cell lines acquire resistance through distinct mechanisms. Furthermore, we show that the KPL-4 T-DM1 resistance can be overcome by treatment with an inhibitor of MDR1, whereas a PI3K inhibitor can rescue PTEN loss–induced resistance in T-DM1–resistant BT-474M1 cells. Our results provide a rationale for developing therapeutic strategies to enhance T-DM1 clinical efficacy by combining T-DM1 and other inhibitors that target signaling transduction or resistance pathways. *Mol Cancer Ther; 17(7); 1441–53. ©2018 AACR.*

Introduction

The *HER2/erbB2* oncogene encodes a 185-kDa transmembrane receptor tyrosine kinase (RTK) that belongs to the EGFR family and regulates proliferation, differentiation, apoptosis, and metastasis (1). *HER2* gene amplification occurs in approximately 20% of breast cancer and is associated with increased disease recurrence and poor prognosis (2). Trastuzumab (Herceptin), a humanized antibody directed against the HER2 extracellular domain (3), is approved for treating HER2-positive breast cancer in the metastatic (4) and adjuvant settings (5). Mechanisms attributed to trastuzumab activity include inhibition of HER2/HER3/PI3K signaling (6, 7), prevention of HER2 ectodomain shedding (8), initiation of G1 arrest via induction of the cyclin-dependent kinase inhibitor $p27^{KIP1}$ (9), and inhibition of angiogenesis (10). In addition, trastuzumab engages Fc receptor-expressing immune effector cells to induce antibody-dependent, cell-mediated cytotoxicity (ADCC; ref. 9).

Despite clinical activity, a proportion of patients do not respond to trastuzumab because of *de novo* or acquired resistance (11). Potential mechanisms of resistance include PTEN loss and enhanced AKT signaling (6), altered receptor–antibody interaction (12), and activation of other RTKs (13). Therefore, identification of new therapeutic agents that are effective in trastuzumab-refractory tumors is key for improving survival of breast cancer patients whose tumors overexpress HER2.

Trastuzumab emtansine (T-DM1, Kadcyla) is an antibody–drug conjugate (ADC) comprised of trastuzumab covalently bound to DM1 via a nonreducible thioether linker (4-[N-maleimidomethyl]cyclohexane-1-carboxylate, MCC). DM1, a maytansine derivative, is a potent antimitotic agent that binds microtubules similar to vinca alkaloids. T-DM1 allows intracellular delivery of DM1 selectively to HER2-overexpressing cancer cells, thereby minimizing exposure of normal tissue to the toxicities of the DM1 component and improving the therapeutic index. In preclinical models, T-DM1 potently inhibits growth of trastuzumab-sensitive and -insensitive HER2-amplified cancer cells (14). In addition, T-DM1 retains the antitumor properties of trastuzumab (15). T-DM1 was first approved by the FDA based on the phase III EMILIA trial (NCT00829166), which demonstrated that T-DM1 significantly prolonged progression-free and overall survival compared with the control arm, lapatinib plus capecitabine, in HER2-positive metastatic breast cancer (mBC) patients previously treated with trastuzumab and a taxane (16). Moreover, treatment with T-DM1 is better tolerated than chemotherapy-containing regimens.

Despite improved clinical outcome, some patients initially respond to T-DM1 treatment but develop disease progression. Primary resistance can also occur (16). Thus, resistance to T-DM1 poses a challenge in therapy for HER2-positive breast cancer. A better understanding of the molecular mechanisms of primary

[1]Department of Translational Oncology, Genentech, Inc., South San Francisco, California. [2]Department of Preclinical and Translational Pharmacokinetics, Genentech, Inc., South San Francisco, California.

Note: Supplementary data for this article are available at Molecular Cancer Therapeutics Online (http://mct.aacrjournals.org/).

Corresponding Author: Guangmin Li, Genentech, Inc., 1 DNA Way, South San Francisco, CA 94080. Phone: 650-467-7570; Fax: 650-225-1411; E-mail: gli@gene.com

doi: 10.1158/1535-7163.MCT-17-0296

and acquired resistance to T-DM1 is particularly important for the development of new therapeutic strategies. To explore mechanisms of acquired resistance to T-DM1, we established resistant cells with a stepwise escalation method and identified different features of T-DM1–resistant cells. Our findings show the complexities of T-DM1 resistance in that our two models showed little overlap in identified resistance mechanisms. The data also suggest possible therapeutic strategies using combinations with inhibitors that target signal transduction resistance pathways for overcoming T-DM1 resistance.

Materials and Methods

Cell lines and reagents

KPL-4 breast cancer cells were a gift from J. Kurebayashi (17). BT-474M1 is an *in vivo*--passaged subline of BT-474 (7). Cells were cultured as previously described (14). Tetracycline (Tet)-free FBS (Hyclone) was used for maintaining BT-474M1 cells infected with inducible shRNA constructs. T-DM1–resistant lines were generated by continuous exposure to increasing concentrations of T-DM1 up to 2 μg/mL. Parental cells are designated KPL-4 P and BT-474M1 P. Established T-DM1–resistant KPL-4 and BT-474M1 pools were maintained in culture with 2 μg/mL T-DM1, hereafter designated as KPL-4 TR and BT-474M1 TR, respectively. TR-1, used for xenograft studies, are resistant cells grown without T-DM1 for 6 months. Cell line authentication was performed at Genetica DNA Laboratories using short tandem repeat loci analysis. The profiles of BT-474M1 parent and TR cells were a 100% match to reference BT-474 (ATCC HTB-20). KPL-4 parent and TR cells were 92.6% and 100% identical to the reference KPL-4 profile. The results support authentication of all lines compared with the reference profiles.

T-DM1, trastuzumab, mu4D5 (murine parent of trastuzumab), anti–IGF-1R 10H5 (18), GDC-0941 (19), and lapatinib were produced at Genentech. Monomethyl auristatin E (MMAE) was from Seattle Genetics; docetaxel from Sigma Aldrich, and cetuximab from Merck. XR9051 (20), Ko143 (21), and PHA665725 (22) were from Tocris; AMD3100 (23) from Sigma, and IGFBP5 was from R&D Systems. Alexa Fluor 488 anti-human IgG was obtained from Molecular Probes. Free DM1 (S-methyl-DM1) was obtained from ImmunoGen. As DM1 has a free sulfhydryl and can oxidize to produce DM1 disulfide dimers or undergo disulfide exchange with cysteine in tissue culture medium (24), the stable S-methyl-DM1 was used.

Cell viability assays

Cells were seeded in 96-well plates and allowed to adhere overnight. Media were removed and replaced with fresh media containing various concentrations of each drug. Cell Titer-Glo (Promega) was added after 5 days, and the luminescent signal measured using an EnVision Multilabel Plate Reader (PerkinElmer). For experiments with different inhibitors, T-DM1 and the inhibitors were added simultaneously. Data are represented as mean ± SEM, with $n = 4$ per treatment group.

Western blotting

Western immunoblot procedures were described previously (14). Antibodies were against EGFR (MBL), HER2 (Neomarkers), PTEN (Santa Cruz Biotechnology), HER3, AKT, phospho-AKT, ERK, phospho-ERK, IGF-1Rβ, MDR1, and β-actin (all from Cell Signaling Technology), DARPP-32 (Epitomics), Met (Upstate Biotechnology), or BCRP (Kamiya Biomedical).

HER2 fluorescence *in situ* hybridization (FISH)

Cells were harvested, embedded in paraffin and formalin-fixed. The PathVysion probe set, HER2 in SpectrumOrange, CEP 17 in SpectrumGreen (Abbott Molecular) was used in the dual-color FISH assay performed according to the manufacturer's protocol. Analysis was performed on an epifluorescence microscope using single interference filter sets for green (FITC), red (Texas red), and blue (DAPI), as well as dual (red/green) and triple (blue, red, green) band pass filters. At least 20 metaphase spreads and 100 interphase nuclei were analyzed in each cell line. Chromosome designation followed ISCN guidelines. Images were captured using the CytoVision software (Genetix). Gene amplification was defined as a HER2/CEP17 FISH ratio signal > 2.2.

Real-time quantitative PCR

Total RNA was extracted using the RNeasy Mini Kit (QIAGEN) according to manufacturer's instructions. Individual primer/probe sets were from Applied Biosystems or designed with Primer Express software (Applied Biosystems). Total RNA (100 ng) was used as template, and Taqman One-Step Universal Master Mix (Applied Biosystems) was used for all reactions. Reactions were performed in a 96-well plate using ABI 7500 Real-Time qPCR System. Gene expression was normalized using HP1BP3 (heterochromatin protein 1, binding protein 3) as the housekeeping gene.

Microarray analysis

Total RNA (3 μg) was converted into double-stranded cDNA using a SuperScript Choice kit (Invitrogen) and a T7-(dT) primer (Biosearch Technologies, Inc.). cDNA was purified using a Sample Cleanup Module kit (Affymetrix) and used to generate biotin-labeled cRNA using an *in vitro* transcription kit (Enzo Diagnostics, Inc.). Labeled cRNA was purified using a Sample Cleanup Module kit. Labeled cRNA (15 μg) was fragmented and hybridized to Human Genome U133 Plus 2.0 Arrays following the manufacturer's protocol. Arrays were washed and stained in the Affymetrix Fluidics station and scanned on GeneChip scanner 3000. Data analysis was performed using the Affymetrix GeneChip operating system and analysis software. Triplicates of each cell line (parental vs. resistant) were analyzed.

siRNA transfection

SMARTpools, individual siRNA oligonucleotides, and nontargeting siRNAs were purchased from Dharmacon/Thermo Scientific. For reverse transfection, Opti-MEM medium was mixed with siRNA to give a final concentration of 25 nmol/L; this was then combined with diluted DharmaFECT 4 (Thermo Scientific). After 20-minute incubation at room temperature, the transfection mixture was aliquoted into 96-well plates. Cells were added to each well containing siRNA and DharmaFECT complex. Forty-eight hours after transfection, cells were treated with T-DM1, and cell viability was measured after 96 hours.

Inducible PTEN shRNA

Doxycycline-inducible PTEN shRNA in BT-474M1 cells was produced via lentiviral transfection with an eGFP-tagged PTEN as described (25). Fluorescence-activated cell sorting was used to select eGFP-positive cells that were collected and pooled 3 days

after infection. Expanded pools were treated with 25 ng/mL doxycycline (BD Clontech) for 3 days, and endogenous PTEN knockdown assessed.

Mouse xenograft studies

The experiments were carried out in accordance with and approved by an Institutional Animal Care and Use Committee. BT-474M1 (5 million cells, plus estrogen supplementation) or KPL-4 (3 million cells) were implanted, in Matrigel, into the number 2/3 mammary fat pad of NCR nude (Taconic Biosciences) or C.B.-17 SCID.bg (Charles River Laboratories) mice, respectively (7, 26). Mice were randomly assigned to groups when tumor volumes reached approximately 150 to 300 mm^3. Tumor volumes were measured twice a week after a single i.v. injection of 5 mg/kg T-DM1 or vehicle (10 mmol/L sodium succinate, 0.02% polysorbate 20, 6% w/v trehalose dihydrate, pH 5.0).

Statistical methods

For *in vitro* drug combination analysis, combination index (CI) values were derived from the Chou and Talalay method (27), using CalcuSyn software (Biosoft). CI < 1 denotes synergy; CI > 1 denotes antagonism; CI ≅ 1 denotes additivity. For *in vivo* xenograft studies, two-sample Student *t* tests, assuming equal variances and two-tailed distribution, were performed to derive *P* values for end-of-study tumor volumes in treated versus control groups. Statistical significance is reached with *P* values < 0.05.

Results

Establishment and characterization of T-DM1–resistant breast cancer cells

To uncover potential resistance mechanisms to T-DM1, we selected trastuzumab-insensitive KPL-4 and trastuzumab-sensitive BT-474M1 breast cancer cells. Both cell lines are HER2 gene–amplified and are 3+ for HER2 expression by immunohistochemistry (IHC), the diagnostic criteria for clinical use of T-DM1. Cells were chronically exposed to increasing concentrations of T-DM1, over a 10-month period, to a final concentration of 2 μg/mL. The doubling time for KPL-4 TR cells was 2-fold slower than that for parental cells. Doubling times for BT-474M1 parental and resistant cells were similar. Figure 1A (KPL-4) and C (BT-474M1) shows representative dose-response curves for T-DM1, S-methyl-DM1, trastuzumab, and other anticancer agents. IC_{50} values for parental KPL-4 and BT-474M1 cells were 0.0043 and 0.056 μg/mL, respectively, whereas KPL-4 TR and BT-474M1 TR were resistant to T-DM1 at concentrations up to 3 μg/mL. Cross-resistance to S-methyl-DM1 and other antimicrotubule agents, MMAE and docetaxel, was demonstrated in KPL-4 TR (Fig. 1A). In contrast, BT-474M1 TR cells retained sensitivity to all 3 antimitotic agents (Fig. 1C). KPL-4 parental cells are insensitive to trastuzumab, which was maintained in KPL-4 TR cells (Fig. 1A). Interestingly, we observed that T-DM1–resistant BT-474M1 cells manifested resistance to trastuzumab, compared with parental cells (Fig. 1C). We also examined the effects of lapatinib, a dual HER2/EGFR kinase inhibitor. KPL-4 TR cells were less sensitive to treatment with lapatinib (Fig. 1A), whereas BT-474M1 parental and resistant cells showed similar sensitivity (Fig. 1C).

We next performed studies to verify resistance in mouse xenograft models. Initial *in vivo* efforts demonstrated poor growth of BT-474M1 TR cells, and lack of T-DM1 resistance in KPL-4 TR cells (due to loss of MDR1, Supplementary Fig. S1; see transporter section below). We therefore used TR-1 cells for *in vivo* studies. We first established that KPL-4 TR-1 and BT-474M1 TR-1 maintained resistance *in vitro* (Fig. 1A and C, first plots). In mouse xenograft studies, KPL-4 P tumors are highly sensitive to T-DM1 ($P = 6.26 \times 10^{-8}$), whereas KPL-4 TR-1 tumors demonstrated complete resistance (Fig. 1B). BT-474M1 P tumors were also sensitive to T-DM1 ($P = 0.0029$, Fig. 1D). BT-474 TR-1 tumors were partially resistant to T-DM1, with complete resistance at the first measurement (day 3) compared with parental cells, where clear separation between vehicle and T-DM1 was observed. Despite slow regrowth of TR-1 tumors, statistical significance (vehicle vs. T-DM1) was not reached ($P = 0.091$). Our findings are similar to a recent report demonstrating partial resistance *in vivo* in 2 of 3 BT-474 T-DM1–resistant clones (28).

Differentially expressed genes in T-DM1–resistant cells

To gain broad understanding on mechanisms of T-DM1 resistance, we employed Affymetrix HG-U133 plus 2.0 arrays comparing gene expression in parental versus resistant lines. We performed cross-comparison of genes that were differentially expressed (>2-fold and $P < 0.05$) between KPL-4 TR and BT-474M1 TR cells (Table 1). Forty-nine genes were upregulated and 10 genes downregulated in common in resistant cells compared with parental cells. Overall, gene expression fold changes in common were modest (approximately 2- to 4-fold). BHLHE41 (basic helix-loop-helix family, member 41 transcription factor) was the most highly upregulated gene in common between KPL-4 TR and BT-474M1 TR cells (up 12.24- and 8.34-fold, respectively). However, siRNA silencing of BHLHE41 in both TR lines did not reverse T-DM1 resistance (Supplementary Fig. S2). BHLHE41 is reported to regulate sleep cycles (29), B- and T-cell development (30), and suppress metastasis (31). However, no role has yet been described in drug resistance. With the exception of BHLHE41, the more highly regulated genes (>5-fold compared with parental cells) were not found in common in both cell lines. We thus decided to focus on each resistant pair separately. Expression changes > 5-fold in resistant versus parental cells are shown in Supplementary Tables S1 and S2. Supplementary Tables S3 and S4 show gene expression changes > 2-fold. The most notable changes were observed in transporters, adhesion molecules, cytokines/chemokines, proteases and phosphatases, and signal transduction pathways.

Role of RTKs and signal transduction pathways in T-DM1 resistance: HER2 expression, binding, and trafficking

As resistant cells were generated by prolonged exposure to T-DM1, a potential mechanism of T-DM1 resistance is loss of the target, HER2. Reduced HER2 levels in KPL-4 TR cells were demonstrated by microarray (Supplementary Table S2), qRT-PCR (Supplementary Fig. S3), and immunoblot (Fig. 2A). To further characterize expression changes, HER2 amplification was assessed by FISH. The ratio of the average HER2 gene copy number to CEP17 (centromeric protein on chromosome 17) gene copy number was 5.8 in KPL-4 parental and 2.9 in KPL-4 TR cells, demonstrating that KPL-4 TR cells had reduced HER2 gene copy number (Fig. 2B). Decreased HER2 cell surface expression was confirmed by flow cytometry analysis (Supplementary Fig. S2). To understand gene copy number at the protein level, immunoblot analysis was performed and compared with a panel of breast cancer cells that express known HER2 levels. The results

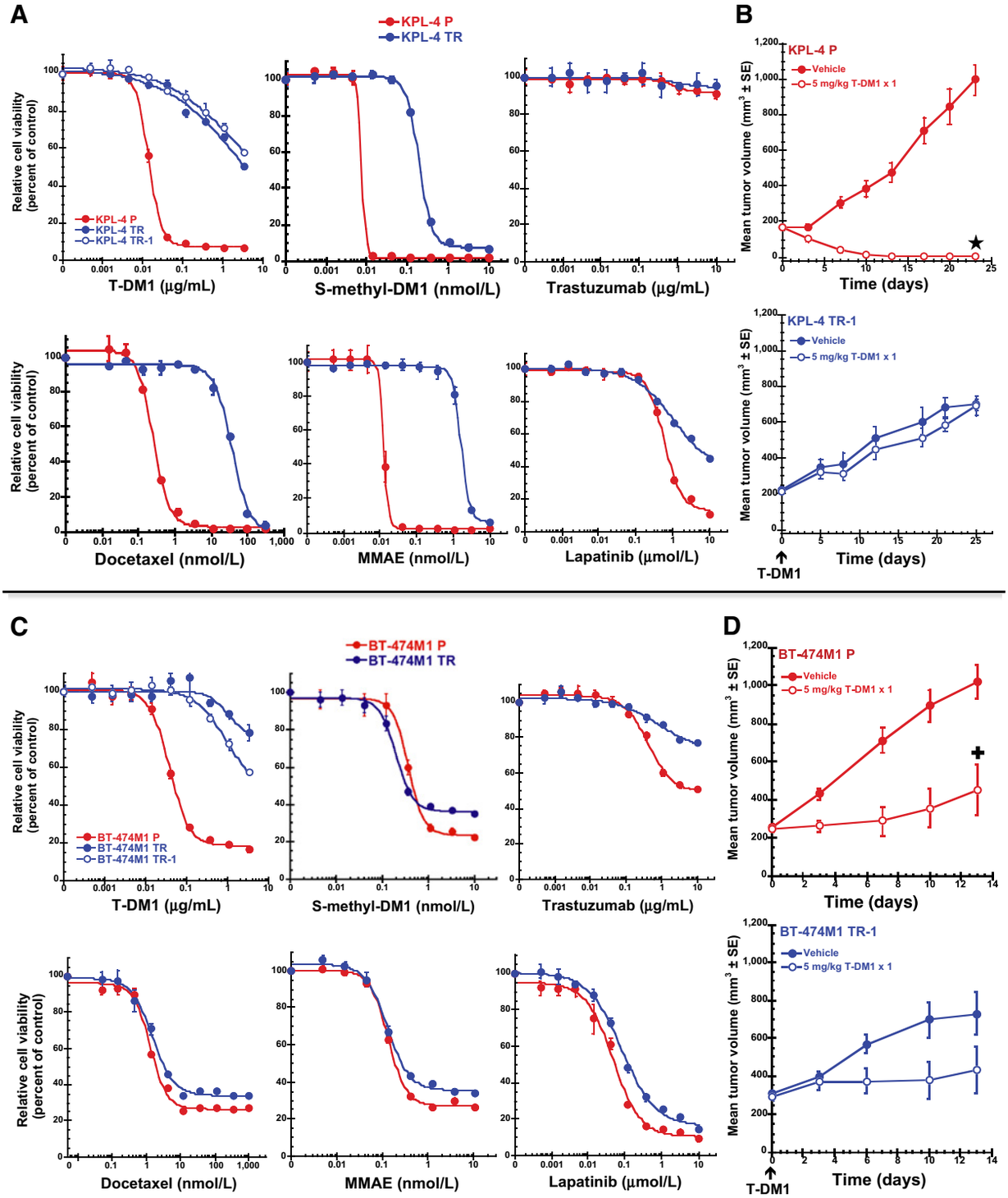

Figure 1.

Response of parental and T-DM1–resistant cells to T-DM1, S-methyl-DM1, MMAE, docetaxel, trastuzumab, and lapatinib *in vitro* and to T-DM1 *in vivo*. KPL-4 parental (P) and resistant cells (TR) *in vitro* (**A**) and *in vivo* (**B**). BT-474M1 parental (P) and resistant (TR) cells *in vitro* (**C**) and *in vivo* (**D**). TR-1 indicates resistant cells grown in the absence of T-DM1 for 6 months. For *in vitro* studies (**A** and **C**), cells were exposed to the indicated concentrations of drug for 5 days ($n = 4$ per group) and cell viability measured by Cell Titer-Glo. For *in vivo* studies (**B** and **D**), mice were treated with T-DM1 (5 mg/kg i.v.; $n = 7$ per group) or vehicle ($n = 7$ per group for KPL-4 P and $n = 9$ per group for BT-474M1 P). All data points represent mean ± SEM; *, $P = 6.26 \times 10^{-8}$ for KPL-4 P, T-DM1 vs. vehicle control; $^{+}$, $P = 0.0029$ for BT-474M1 P, T-DM1 vs. vehicle control. Statistical significance (T-DM1 vs. vehicle control) was not reached for the resistant models ($P = 0.691$ for KPL-4 TR-1; $P = 0.0911$ for BT-474M1 TR-1).

Table 1. Gene expression changes in common (>2-fold change and $P < 0.05$) between KPL-4 and BT-474M1 TR vs. parental cells

Affymetrix ID	Symbol	Description	KPL-4 TR vs. parental		BT-474M1 TR vs. parental	
			Fold change	Adjusted *P* value	Fold change	Adjusted *P* value
204333_s_at	AGA	Aspartylglucosaminidase	2.35	4.51E–08	2.25	3.71E–07
226576_at	ARHGAP26	Rho GTPase-activating protein 26	4.87	6.73E–09	3.73	3.64E–07
221530_s_at	BHLHE41	Basic helix-loop-helix family, member e41	12.24	1.08E–13	8.34	1.42E–11
239697_x_at	C3orf67	Chromosome 3 open reading frame 67	2.28	7.16E–06	2.17	3.97E–05
234990_at	CBX5	Chromobox homolog 5 (HP1 alpha homolog, Drosophila)	2.20	2.25E–04	2.16	5.73E–04
219529_at	CLIC3	Chloride intracellular channel 3	–16.06	1.28E–14	–2.46	5.81E–07
221730_at	COL5A2	Collagen, type V, alpha 2	2.15	4.76E–08	7.46	6.31E–13
214336_s_at	COPA	Coatomer protein complex, subunit alpha	2.83	9.04E–05	2.61	4.51E–04
201117_s_at	CPE	Carboxypeptidase E	4.23	1.40E–10	2.10	4.22E–06
219049_at	CSGALNACT1	Chondroitin sulfate N-acetylgalactosaminyltransferase 1	2.14	4.36E–05	3.10	1.24E–06
204971_at	CSTA	Cystatin A (stefin A)	4.25	1.47E–08	4.24	7.80E–08
209617_s_at	CTNND2	Catenin (cadherin-associated protein), delta 2 (neural plakophilin-related arm-repeat protein)	–16.38	8.38E–16	–2.74	1.60E–08
218976_at	DNAJC12	DnaJ (Hsp40) homolog, subfamily C, member 12	4.28	4.35E–11	2.58	1.01E–07
209457_at	DUSP5	Dual specificity phosphatase 5	2.02	1.54E–08	2.62	1.30E–09
200878_at	EPAS1	Endothelial PAS domain protein 1	2.21	1.17E–08	2.33	2.74E–08
221959_at	FAM110B	Family with sequence similarity 110, member B	–4.09	6.91E–12	–2.09	3.14E–07
226863_at	FAM110C	Family with sequence similarity 110, member C	3.22	2.35E–11	2.87	8.25E–10
203987_at	FZD6	Frizzled homolog 6 (Drosophila)	2.96	7.25E–10	2.31	1.30E–07
223204_at	FAM198B	Family with sequence similarity 198, member B	31.46	8.18E–18	2.09	1.64E–07
218885_s_at	GALNT12	UDP-N-acetyl-alpha-D-galactosamine:polypeptide N-acetylgalactosaminyltransferase 12 (GalNAc-T12)	6.65	4.96E–13	2.36	2.14E–07
209276_s_at	GLRX	Glutaredoxin (thioltransferase)	4.21	1.11E–11	2.07	7.01E–07
206917_at	GNA13	Guanine nucleotide binding protein (G protein), alpha 13	2.01	1.03E–02	2.13	9.50E–03
204983_s_at	GPC4	Glypican 4	2.20	1.72E–07	2.69	4.43E–08
209398_at	HIST1H1C	Histone cluster 1, H1c	5.04	2.47E–13	2.87	1.04E–09
211958_at	IGFBP5	Insulin-like growth factor binding protein 5	–2.00	1.46E–04	–5.89	6.31E–09
210904_s_at	IL13RA1	Interleukin 13 receptor, alpha 1	3.65	2.96E–09	2.26	4.88E–06
215177_s_at	ITGA6	Integrin, alpha 6	3.55	2.39E–10	2.18	8.62E–07
226535_at	ITGB6	Integrin, beta 6	2.38	3.08E–08	2.46	9.28E–08
217388_s_at	KYNU	Kynureninase (L-kynurenine hydrolase)	2.16	1.27E–08	2.73	2.08E–09
210732_s_at	LGALS8	Lectin, galactoside-binding, soluble, 8	7.72	3.08E–14	2.26	1.01E–07
202501_at	MAPRE2	Microtubule-associated protein, RP/EB family, member 2	2.27	3.30E–07	2.24	1.46E–06
205018_s_at	MBNL2	Muscleblind-like 2 (Drosophila)	2.59	3.86E–05	3.11	1.44E–05
210136_at	MBP	Myelin basic protein	2.72	3.56E–10	2.72	2.73E–09
1553602_at	MUCL1	Mucin-like 1	–6.48	1.67E–14	–2.03	1.15E–07
202180_s_at	MVP	Major vault protein	2.03	1.63E–07	2.59	1.75E–08
227971_at	NRK	Nik-related kinase	–2.38	5.69E–05	–5.58	5.10E–08
205078_at	PIGF	Phosphatidylinositol glycan anchor biosynthesis, class F	2.03	3.10E–08	2.07	1.01E–07
230076_at	PITPNM3	PITPNM family member 3	–2.05	4.48E–06	–3.32	2.95E–08
210946_at	PPAP2A	Phosphatidic acid phosphatase type 2A	3.05	9.79E–10	2.03	1.84E–06
204364_s_at	REEP1	Receptor accessory protein 1	–2.34	5.72E–09	–2.75	3.68E–09
226021_at	RDH10	Retinol dehydrogenase 10 (all-trans)	4.65	2.10E–11	2.73	5.20E–08
219263_at	RNF128	Ring finger protein 128	21.29	1.85E–13	2.11	1.07E–04
232231_at	RUNX2	Runt-related transcription factor 2	6.89	2.28E–14	2.32	2.53E–08
204855_at	SERPINB5	Serpin peptidase inhibitor, clade B (ovalbumin), member 5	6.26	1.28E–13	3.59	2.29E–10
201312_s_at	SH3BGRL	SH3 domain binding glutamic acid-rich protein like	8.77	1.70E–14	2.81	6.65E–09
230493_at	SHISA2	Shisa homolog 2 (Xenopus laevis)	–3.85	9.21E–10	–3.11	5.56E–08
217678_at	SLC7A11	Solute carrier family 7, (cationic amino acid transporter, y+ system) member 11	3.16	6.37E–04	2.89	2.38E–03
204955_at	SRPX	Sushi-repeat-containing protein, X-linked	6.33	2.51E–12	2.04	5.30E–06
226932_at	SSPN	Sarcospan (Kras oncogene-associated gene)	5.03	7.06E–11	3.83	7.21E–09
203217_s_at	ST3GAL5	ST3 beta-galactoside alpha-2,3-sialyltransferase 5	3.19	2.67E–12	2.48	7.53E–10
202786_at	STK39	Serine threonine kinase 39 (STE20/SPS1 homolog, yeast)	2.70	2.65E–09	2.97	5.23E–09
203767_s_at	STS	Steroid sulfatase (microsomal), isozyme S	3.23	3.60E–10	2.03	1.49E–06
242093_at	SYTL5	Synaptotagmin-like 5	3.61	4.55E–10	2.55	1.83E–07
209153_s_at	TCF3	Transcription factor 3 (E2A immunoglobulin enhancer binding factors E12/E47)	–3.92	2.21E–11	–2.33	1.05E–07
213258_at	TFPI	Tissue factor pathway inhibitor (lipoprotein-associated coagulation inhibitor)	28.56	1.04E–16	2.23	4.02E–07
231579_s_at	TIMP2	TIMP metallopeptidase inhibitor 2	2.74	2.29E–10	4.66	5.46E–12
210260_s_at	TNFAIP8	Tumor necrosis factor, alpha-induced protein 8	3.48	1.13E–08	2.56	1.87E–06
214329_x_at	TNFSF10	Tumor necrosis factor (ligand) superfamily, member 10	7.51	4.46E–15	2.14	3.52E–08
226208_at	ZSWIM6	Zinc finger, SWIM-type containing 6	3.80	1.38E–11	2.01	5.71E–07

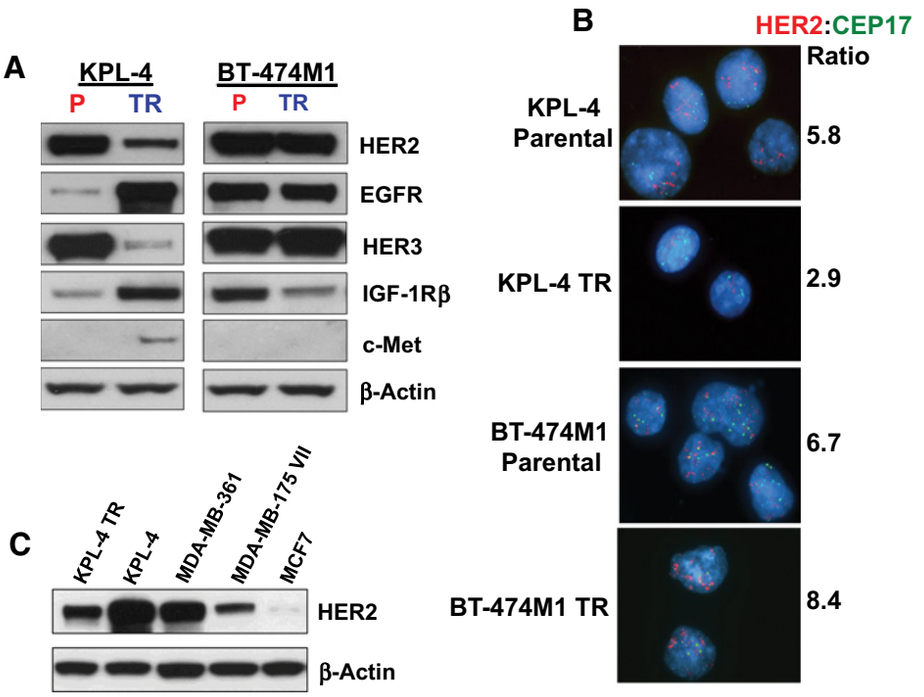

Figure 2.
Expression of RTKs in T-DM1–resistant cells. **A,** Immunoblot analysis of basal-level expression of EGFR, HER2, HER3, c-Met, and IGF-1Rβ in whole cell lysates from parental (P) and resistant (TR) cells. **B,** FISH analysis of HER2 amplification in parental and T-DM1–resistant cells. Interphase nuclei showing HER2 signals (red) compared with CEP17 (green). A ratio of HER2:chromosome 17 signal > 2.2 indicates HER2 gene amplification. **C,** HER2 expression by Western blot analysis in KPL-4 TR cells compared with known standard cell line panel (IHC scores: MCF7 = 0; MDA-MB-175-VII = 1+; MDA-MB-361 = 2+; KPL-4 = 3+).

demonstrate that KPL-4 TR cells did not lose HER2 expression, but rather express HER2 at the 1+ to 2+ level (Fig. 2C). These findings suggest that, during chronic exposure, T-DM1 eliminates cells expressing the highest HER2 levels. We were unsuccessful reintroducing HER2 overexpression into KPL-4 TR cells, despite using a number of different transfection methods. Given preclinical and clinical data demonstrating the requirement for HER2 overexpression for T-DM1 activity (14, 32), we did not pursue this further. In contrast, there was no decrease in HER2 protein level or HER2:CEP17 ratio in BT-474M1 TR compared with parental cells (Fig. 2A and B, respectively), or in HER2 cell surface expression or trastuzumab binding as determined by flow cytometry (Supplementary Fig. S4) and immunofluorescence microscopy (Supplementary Fig. S5). Therefore, the mechanisms of acquired resistance in this setting cannot be attributed to decreased HER2.

Uptake and processing of T-DM1 in resistant cells

To investigate differences in uptake and/or processing of T-DM1, we performed studies with two radiolabeled probes: ^{125}I-trastuzumab for assessing antibody internalization, and trastuzumab-[^{3}H]-DM1 for tracking DM1, as described by Erickson and colleagues (33). Although the kinetics of ^{125}I-trastuzumab uptake in BT-474M1 TR cells were delayed compared with parental cells (Supplementary Fig. S6A, left), by 24 hours, the total radioactivity in both parent and TR cells was equal. In cells exposed to trastuzumab-[^{3}H]-DM1, the amount of total and fractionated (soluble and precipitable) DM1 was not different in BT-474M1 parent versus TR (Supplementary Fig. S6A, right), indicating no differences in processing in the resistant cells. ^{125}I-trastuzumab uptake in KPL-4 TR was lower compared with parental cells (Supplementary Fig. S6B, left), likely a result of decreased HER2. Similarly, decreased intracellular DM1 was observed in KPL-4 TR (Supplementary Fig. S6B, right), with KPL-4 parental cells showing similar processing as reported for other HER2-positive breast cancer lines (33).

Altered expression of RTKs

Activation of alternative signaling pathways confers resistance to targeted therapeutics (34). Therefore, we evaluated expression of additional RTKs (Fig. 2A; Supplementary Fig. S3) and ligands (Supplementary Fig. S3) by Western blotting and qRT-PCR. Expression of EGFR, and to a lesser extent, IGF-1Rβ and c-Met, was elevated in KPL-4 TR relative to parental cells, whereas HER3 expression was decreased (Fig. 2A; Supplementary Table S2). Both IGF-1Rβ and c-Met are reported to mediate trastuzumab resistance in preclinical models (35, 36). Although KPL-4 are innately resistant to trastuzumab *in vitro*, we nevertheless tested inhibitors of IGF-1Rβ and c-Met in the context of T-DM1 resistance and found that neither RTK mediated resistance in KPL-4 TR cells (Supplementary Fig. S7). BT-474M1 TR cells did not show differences in RTK expression, with the exception of slightly decreased IGF-1Rβ.

As both EGFR and TGFα were elevated in KPL-4 TR cells (Fig. 2; Supplementary Fig. S3), we investigated the role of EGFR in T-DM1 resistance. Studies using siRNA to deplete EGFR showed that EGFR expression did not mediate resistance to T-DM1 (Supplementary Fig. S8A). Moreover, addition of exogenous TGFα to KPL-4 parental cells did not cause T-DM1 resistance (Supplementary Fig. S9B). Additional studies investigated effects of cetuximab, an EGFR-directed antibody, alone or in combination with T-DM1. Despite upregulated receptor and ligand, addition of cetuximab alone did not inhibit cell growth and did not sensitize KPL-4 TR cells when added with T-DM1 (Supplementary Fig. S8B).

Our qRT-PCR studies (Supplementary Fig. S3) also demonstrated increased expression of HER4 and one of its ligands, neuregulin (as a pan-NRG probe was used, the specific isoform

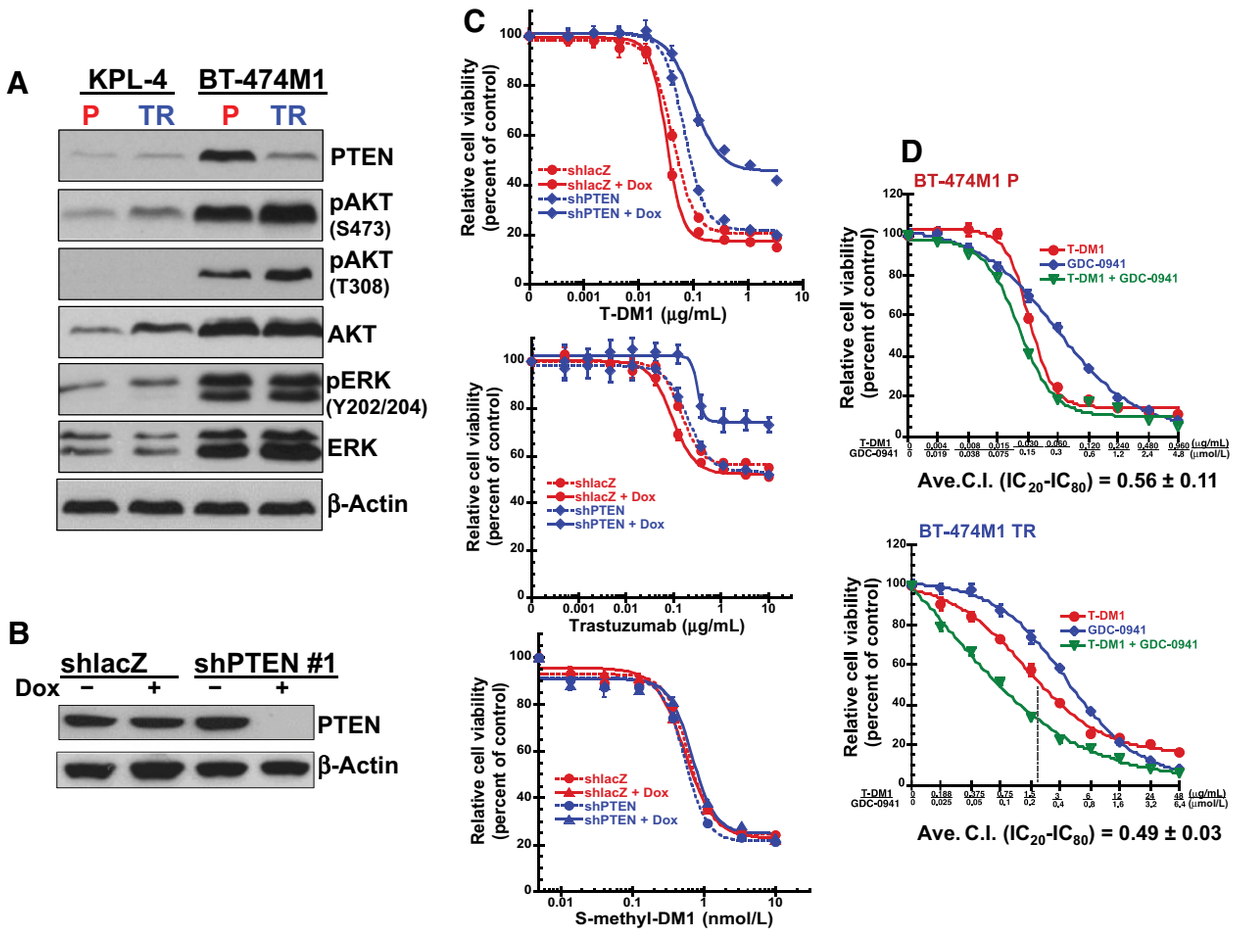

Figure 3.

T-DM1 resistance mediated by PTEN loss and activated AKT in BT-474M1 TR cells can be reversed with the PI3K inhibitor GDC-0941. **A,** Reduced PTEN expression and increased phosphorylated AKT in T-DM1–resistant BT-474M1 cells compared with KPL-4 cells; **B** and **C,** PTEN silencing by PTEN shRNA results in decreased sensitivity to T-DM1. BT-474M1 parental cells transfected with control LacZ shRNA or PTEN shRNA clone #1 were cultured in the presence or absence of doxycycline (25 ng/mL) for 72 hours and harvested for Western blot analysis (**B**) or exposed to T-DM1, trastuzumab, or S-methyl-DM1 for cell viability assessment at 5 days (**C**). As PTEN shRNA clone #3 gave similar results, only clone #1 is shown. **D,** BT-474M1 parental and resistant cells were treated with T-DM1, GDC-0941, or the combination using the Chou and Talalay fixed IC_{50} ratio method. Cells were treated for 5 days, followed by cell viability assessment. For **C** and **D**, each treatment group consisted of four replicates. Data points represent mean ± SEM. CI < 1 denotes synergy. Note the different T-DM1 concentrations for parent vs. resistant cells. As the Chou and Talalay method requires complete dose-response curves to generate CI values, high concentrations of T-DM1 were required for BT-474M1 TR cells, up to 48 vs. 2 μg/mL used to develop acquired resistance (the gray dotted line denotes 2 μg/mL T-DM1). The TR cells still show high relative resistance compared with parental cells.

was not identified). Because NRG is a reported resistance factor for multiple anticancer agents (26, 37, 38), we investigated the potential role of this receptor–ligand interaction. Using a ligand-blocking HER4 antibody (38), we were unable to resensitize KPL-4 TR cells to T-DM1 (Supplementary Fig. S9D).

PTEN deficiency as a resistance mechanism in BT-474M1 cells

Part of our investigation into RTKs included immunoblot analysis for signal transduction pathways downstream of HER2 (Fig. 3A), revealing decreased PTEN expression in BT-474M1 TR cells. As PTEN is a negative regulator of the PI3K pathway, an important survival pathway, and PTEN deficiency is a resistance mechanism to trastuzumab-based therapy (6), we hypothesized that PTEN might play a role in resistance to T-DM1. We first examined if re-expression of PTEN restored sensitivity of BT-474M1 TR cells to T-DM1. We were unable to reintroduce PTEN into BT-474M1 TR cells as the PTEN-transfected cells eventually died. We then used lentivirus-mediated delivery of PTEN shRNA to deplete PTEN in BT-474M1 parental cells. Immunoblot analysis showed depletion of PTEN protein using PTEN-directed shRNA clone 1 (Fig. 3B; Supplementary Fig. S10). We next examined response of PTEN knockdown cells to T-DM1. Ablation of PTEN expression in parental cells led to reduced activity of T-DM1 (Fig. 3C, top). As expected, PTEN knockdown also conferred resistance to trastuzumab (Fig. 3C, middle), which is in agreement with previous reports (39). However, sensitivity to S-methyl-DM1 was similar in shPTEN cells compared with control cells (Fig. 5C, bottom). These data provide evidence that resistance to T-DM1 in BT-474M1 TR cells was associated with reduced PTEN levels.

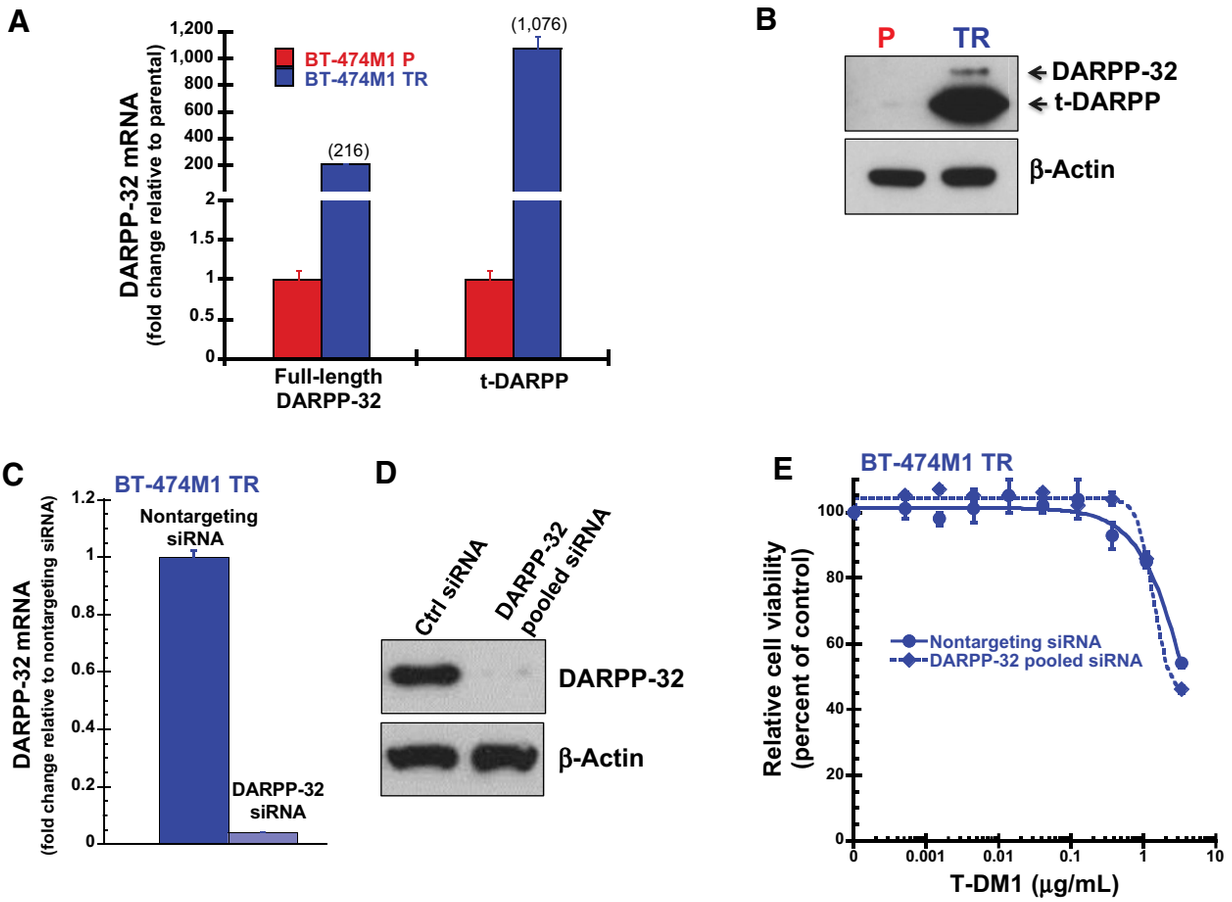

Figure 4.

DARPP-32 overexpression does not contribute to T-DM1 resistance in BT-474M1 TR cells. Expression of both DARPP-32 and t-DARPP is increased in BT-474M1 TR cells, demonstrated by qRT-PCR (**A**) and immunoblot (**B**). Depletion of DARPP-32 by siRNA does not sensitize BT-474M1 TR cells to T-DM1. BT-474M1 TR cells were transfected with either control siRNA or pooled DARPP-32 siRNA. Cell lysates were collected at 72 hours for mRNA (**C**) or protein (**D**) analysis. Concomitantly, cells were treated with T-DM1 48 hours after transfection, and cell viability measured after 4 days (**E**). Each treatment group in cell viability assays consisted of 4 replicates. qRT-PCR analyses were performed with triplicate samples. Data points represent mean ± SEM.

Loss of PTEN results in constitutive activation of PI3K/AKT (6). In BT-474M1 TR cells, reduced PTEN expression led to increased levels of phosphorylated AKT (Fig. 3A). Therefore, we reasoned that inactivation of PI3K may rescue T-DM1 resistance from PTEN deficiency. Combining T-DM1 with the pan-PI3K inhibitor GDC-0941 (19) was more synergistic in BT-474M1 TR cells (Fig. 3D, top) than in parental cells (Fig. 3D, bottom), with average CI values of 0.49 and 0.56, respectively. These data demonstrate that PI3K inhibition enhances sensitivity to T-DM1 to a greater degree in PTEN low T-DM1–resistant cells.

Upregulated DARPP-32 is not a resistance mechanism

The most highly upregulated gene in BT-474M1 TR cells was dopamine and cyclic AMP-regulated phosphoprotein, DARPP-32, also known as protein phosphatase 1 regulatory subunit 1B or PPP1R1B (ref. 40; 56-fold increase; Supplementary Table S1). Both DARPP-32 and its truncated variant, t-DARPP, are recognized by the same probe sets on microarray chips. Further analysis by qRT-PCR and immunoblot showed that expression of both forms was increased relative to parental cells, with t-DARPP the predominant form (Fig. 4A and B). DARPP-32 and t-DARPP are reported to mediate trastuzumab resistance in breast cancer cells (40). To examine if DARPP-32 upregulation was sufficient to confer T-DM1 resistance, BT-474M1 TR cells were transfected with DARPP-32 pooled siRNA that targeted both the full-length and truncated forms. Cells transfected with nontargeting siRNA were used as control. mRNA and protein analysis (Fig. 4C and D) confirmed reduction in DARPP-32 levels in TR cells transfected with DARPP-32 siRNA. However, DARPP-32 depletion did not restore T-DM1 sensitivity (Fig. 4E), indicating that DARPP-32 did not mediate T-DM1 resistance in BT-474M1 TR cells.

In addition to DARPP-32, we investigated the role of two other differentially regulated genes in BT-474M1 TR, *IGFBP5* and *CXCR4* (5.7-fold decrease and 8.2-fold increase, respectively, average of two probes; Supplementary Table S1), which could be functionally implicated in resistance. Exposing cells to exogenous IGFBP5, or to a selective CXCR4 inhibitor, AMD3100 (23), did not reverse resistance of BT-474M1 TR cells to T-DM1 (Supplementary Fig. S11A and S11B).

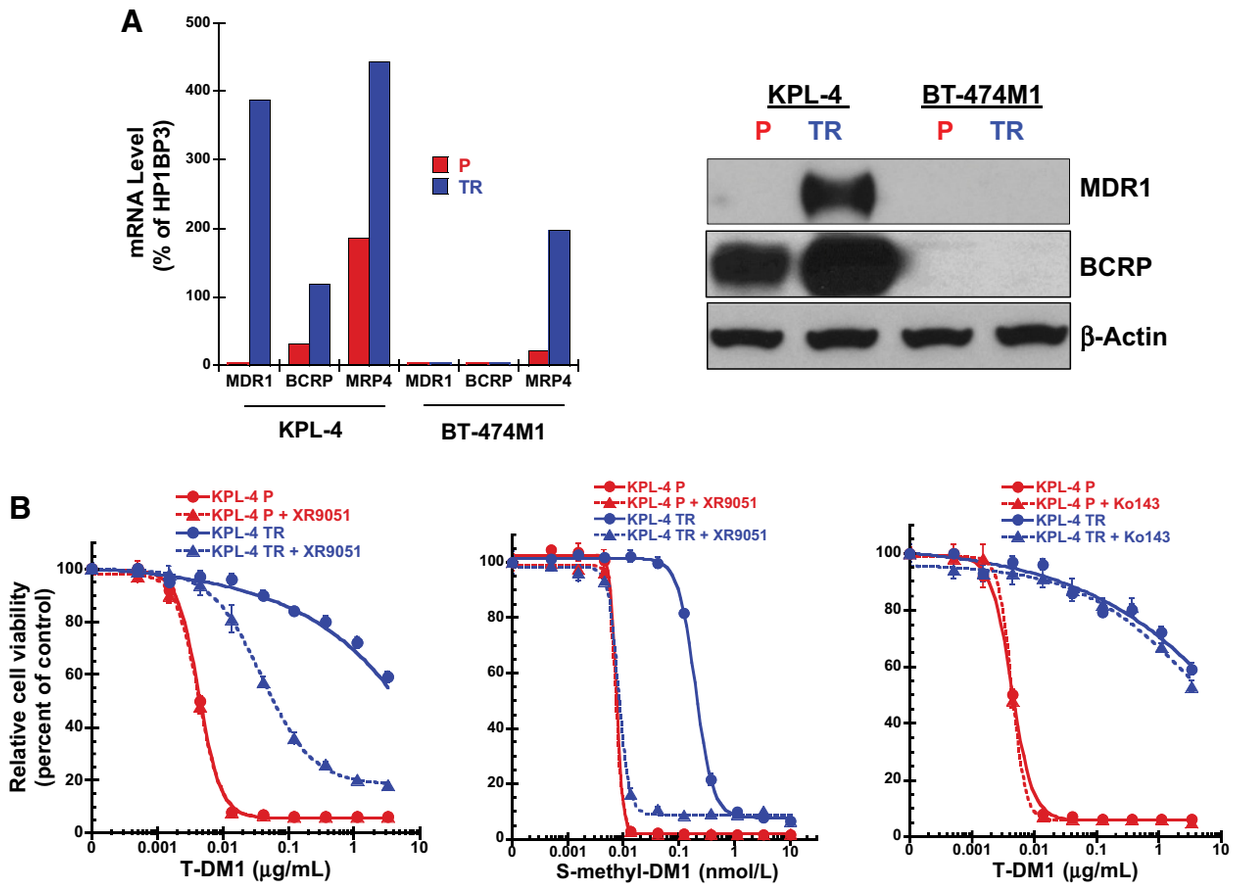

Figure 5.

Expression and function of upregulated drug resistance transporters in T-DM1–resistant cells. **A,** qRT-PCR (left) and immunoblots (right) demonstrate elevated MDR1 and BCRP expression in KPL-4 TR, and increased MRP4 in both KPL-4 and BT-474M1 TR lines (due to the poor quality of MRP4 antibodies, only qRT-PCR for MRP4 is shown). Samples for mRNA and protein analysis were derived from the same flask of P or TR cells. **B,** MDR1 inhibition by XR9051 (300 nmol/L) circumvents T-DM1 and S-methyl-DM1 resistance in KPL-4 TR cells, whereas inhibition of BCRP by Ko143 (200 nmol/L) has no effect. Data points represent mean ± SEM, with $n = 4$ per group.

Role of transporters in T-DM1 resistance

A number of transporters of the ATP-binding cassette (ABC) and solute carrier (SLC) families were upregulated in both TR cell lines (Supplementary Tables S3 and S4). In KPL-4 TR cells, microarray data showed highly increased expression of ABCB1 (MDR1), with moderate increases in ABCC1 (MRP1), ABCC4 (MRP4), ABCC10 (MRP7), and ABCG2 (BCRP/breast cancer resistance protein). In contrast, modest upregulation of ABCC4, ABCC11 (MRP8), ABCD3, and ABCG1 was observed in BT-474M1 TR cells. To verify expression, qRT-PCR was performed for transporters with reported functions in cancer drug resistance (41). Increased expression of MDR1 and BCRP was confirmed in KPL-4 TR cells by qRT-PCR and immunoblot analysis, and increased MRP4 was confirmed in KPL-4 TR and BT-474M1 TR cells (Fig. 5A). We assessed additional MRP transporters (MRP1, MRP2, and MRP3) by qRT-PCR and demonstrated modest to no increase in KPL-4 TR and BT-474M1 TR cells (Supplementary Fig. S12).

To investigate the role of increased MDR1 or BCRP in T-DM1 resistance in KPL-4 TR cells, we assessed whether pharmacologic inhibition would restore T-DM1 sensitivity. Inhibition of MDR1 with XR9051, a potent and selective MDR1 inhibitor (20), resulted in substantial reversal of resistance to both T-DM1 and S-methyl-DM1 (Fig. 5B), whereas XR9051 had no effect on response of KPL-4 parental cells to either agent. Given the increase in both MDR1 and EGFR in KPL-4 TR cells, we then investigated whether combined inhibition would further reverse resistance. Addition of cetuximab with XR9051 did not enhance sensitivity to T-DM1 compared with XR9051 alone (Supplementary Fig. S8B). Despite elevated BCRP, the BCRP inhibitor Ko143 (21) did not resensitize KPL-4 TR cells to T-DM1 (Fig. 5B, right). XR9051 and Ko143 alone had no effect on cell viability (Supplementary Fig. S13).

As there is no selective MRP4 inhibitor available, we used siRNA knockdown to investigate the role of MRP4 in T-DM1 resistance. Although both TR cell lines showed increased MRP4, depletion by individual or pooled siRNA oligonucleotides did not reduce resistance to T-DM1 (Supplementary Figs. 14 and 15). Although we observed variability in knockdown efficiency, MRP4 siRNA #1 showed the greatest depletion (80% in BT-474M1 TR and 70% in KPL-4 TR) but with no reversal of resistance in either cell line. Taken together, these data support the mechanisms of T-DM1

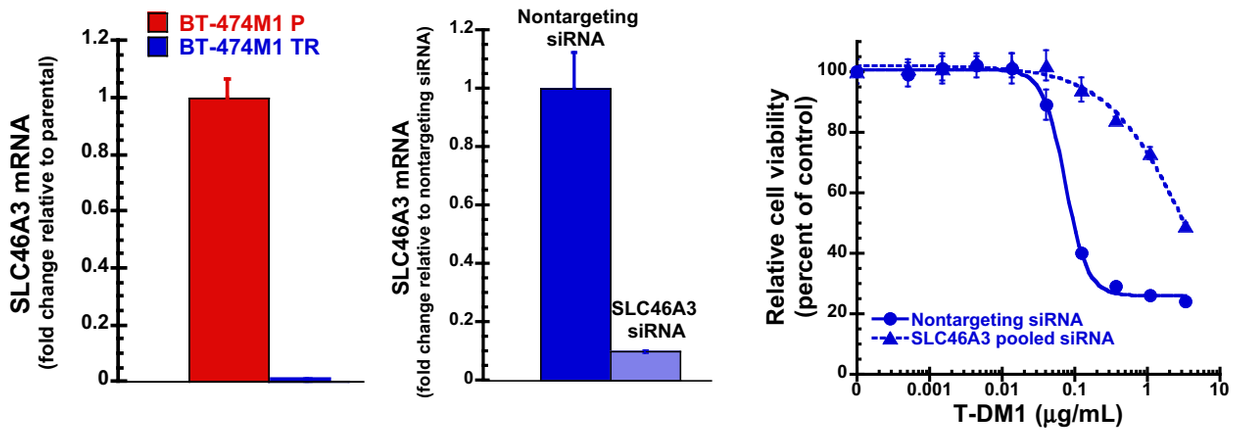

Figure 6.

Role of the lysosomal transporter SLC46A3 in T-DM1 resistance in BT-474M1 cells. SLC46A3 expression is profoundly reduced in BT-474M1 TR cells (left). siRNA knockdown of SLC46A3 (using pooled siRNA) in BT-474M1 parental cells (middle) results in reduced sensitivity to T-DM1 (right). Data points represent mean ± SEM, with $n = 3$ per group for mRNA analysis and $n = 4$ for cell viability assay.

resistance in KPL-4 TR cells as decreased HER2 and increased MDR1 expression.

SLC transporter gene expression changes were abundant in TR cells. BT-474M1 TR cells showed changes (up or down) in 16 SLC family members, whereas 31 SLC genes were differentially expressed in KPL-4 TR cells. As fold changes were modest, most notably in BT-474M1 TR cells, and because the function of SLCs in cancer drug resistance is not established (42), we initially did not follow up on these observations. Recently, Hamblett and colleagues (43) reported that loss of the lysosomal transporter SLC46A3 mediates resistance to maytansinoid-containing ADCs with noncleavable linkers. As the resistance mechanisms in BT-474M1 cells were not completely defined, we performed qRT-PCR for SLC46A3 in our resistant cells, despite no evidence for SLC46A3 loss from microarray data. Interestingly, SLC46A3 expression was lost in BT-474M1 TR cells (Fig. 6, left). Modestly reduced expression was observed in KPL-4 TR cells (−2.79 fold by microarray, Supplementary Table S4, but < 2-fold decrease by qRT-PCR, Supplementary Fig. S16). A role for SLC46A3 in T-DM1 resistance in BT-474M1 parental cells was then verified by using individual and pooled oligonucleotides for siRNA knockdown (Fig. 6, middle; Supplementary Fig. S17), which resulted in resistance to T-DM1 (Fig. 6, right), to a level similar to BT-474M1 TR cells.

Discussion

Understanding mechanisms of drug resistance in preclinical models poses challenges due to the complex nature of resistance and compensatory pathways, as well as the use of different tumor cell models with diverse genetic backgrounds. Moreover, identifying resistance mechanisms for ADCs is complicated by the nature of the drug itself, in that there are multiple components (antibody, linker, cytotoxic agent) to consider. One of the mechanisms by which tumors acquire drug resistance is increased expression of ABC transporters, which actively efflux anticancer drugs out of cells. Expression of MDR1, MRP4, and BCRP was increased in KPL-4 TR, and MRP4 elevated in BT-474M1 TR, compared with parental cells. Inhibition of MDR1 with a selective inhibitor restored sensitivity to T-DM1 and DM1, whereas BCRP or MRP4 inhibition did not. Despite increased expression of multiple drug transporters in our resistant cells, collective data support a role only for MDR1 and MRP1 (44). Trock and colleagues found that breast cancer patients with tumors expressing MDR1 were 3 times more likely to fail to respond to chemotherapy than patients whose tumors were MDR1 negative (26). The clinical significance of MDR1 or MRP1 as mechanisms of drug resistance in patients receiving T-DM1 treatment has not been established. It is unclear if patients with *de novo* resistance to T-DM1 have higher MDR1 expression or whether acquisition of T-DM1 resistance after therapy parallels increased expression of MDR1.

In addition to MDR1 upregulation, a second predominant resistance mechanism in KPL-4 TR cells was decreased HER2 expression. These results are consistent with reported resistance mechanisms for MMAE-containing ADCs targeting CD22 and CD79b (45), as well as CD30 (46), and suggest common resistance alterations among some models. A previous report described *in vitro*–acquired resistance to a trastuzumab–maytansinoid ADC (44) in MDA-MB-361 and JIMT1 cells, both of which are HER2 2+ by IHC, and thus less clinically relevant for T-DM1. JIMT1 cells also express MUC4, a glycoprotein that interferes with trastuzumab binding to HER2 (47), which complicates interpretation of trastuzumab and T-DM1 activity. Increased MRP1 and decreased HER2 were the primary resistance mechanisms for JIMT1 and MDA-MB-361 cells. Global alterations in proteins involved in posttranslational modification, vesicle transport, and trafficking were also described.

Following ADC catabolism and/or linker cleavage in the lysosomal compartment, transport of free drug or catabolites across the lysosomal membrane is required for ADC activity. A unique lysosomal transporter, SLC46A3, was recently shown to transport catabolites of maytansinoid-containing ADCs with noncleavable linkers (43). Although expression changes were not observed in our Affymetrix study, we demonstrated loss of SLC46A3 expression by qRT-PCR in BT-474M1 TR cells. Furthermore, silencing of SLC46A3 expression conferred partial resistance to T-DM1 in parental cells, supporting a role for SLC46A3 loss in T-DM1 resistance. As the sole catabolite of T-DM1 is lysine-MCC-DM1

(33), these data also provided an explanation for BT-474M1 TR cells retaining sensitivity to free DM1. Acquired T-DM1 resistance in BT-474 cells was recently reported to result from T-DM1 accumulation in lysosomes, mediated by decreased lysosomal proteolytic activity (28). Alterations in specific lysosomal proteins were not described.

Approximately 50% of patients with breast cancer have a mutation in or loss of at least one copy of the PTEN gene, which results in activation of PI3K signaling (48). Nagata and colleagues reported that decreased PTEN expression resulted in activation of the PI3K/AKT pathway and inhibition of trastuzumab-mediated growth arrest in HER2-overexpressing breast cancer cells (6). Furthermore, they demonstrated that PI3K inhibitors rescued trastuzumab resistance in PTEN-deficient cells *in vitro* and *in vivo*. Importantly, patients with PTEN-deficient HER2-overexpressing breast tumors had significantly worse responses to trastuzumab-based therapy than those with tumors expressing normal PTEN (48). Berns and colleagues used large-scale RNA interference screens in BT-474 cells and identified PTEN as the only gene whose knockdown resulted in trastuzumab resistance (39). Our data revealed that BT-474M1 TR cells expressed reduced levels of PTEN compared with parental cells. Moreover, decreased PTEN reduced sensitivity to T-DM1. Interestingly, BT-474M1 TR cells were cross-resistant to trastuzumab, but maintained sensitivity to free DM1. Thus, it is likely that T-DM1 resistance is partially due to resistance to trastuzumab. In addition, we found that T-DM1 combined with the PI3K inhibitor GDC-0941 synergistically inhibited BT-474M1 TR cell growth. The combination also demonstrated enhanced growth inhibition in parental cells. These data indicate that PI3K inhibition can sensitize T-DM1–resistant BT-474M1 cells. Combining T-DM1 with inhibitors that target signaling transduction pathways might be a promising strategy to improve T-DM1 efficacy and circumvent resistance. The combination of T-DM1 with PI3K inhibitors is currently under clinical investigation.

In addition to the molecular alterations discussed above, we observed increased expression of a number of RTKs—IGF-1Rβ, c-Met, and EGFR—that are implicated in trastuzumab resistance (35, 36, 49). Functional studies, however, failed to demonstrate roles in T-DM1 resistance. We performed similar studies investigating potential roles in T-DM1 resistance for additional genes that were differentially regulated. Upregulation of DARPP-32, CXCR4, as well as decreased IGFBP5 did not mediate T-DM1 resistance. Recently, defects in cyclin B1 induction were described to play a role in acquired T-DM1 resistance in HCC1954, HCC1419, and SK-BR-3 breast cancer cells (50). These findings highlight the complex nature of molecular alterations resulting from chronic ADC exposure as well as the importance of assessing function of each molecule in the context of resistance.

In summary, our models provide a valuable tool for investigating molecular mechanisms of acquired resistance to T-DM1. It will be important to determine if the features of T-DM1 resistance observed in our studies are present in breast cancer patients who progress during T-DM1 treatment. Collective data from different T-DM1–resistant models indicate that mechanisms of acquired resistance are model dependent (28, 43, 44, 50). Thus, investigating markers of T-DM1 resistance in patients will be complex. Moreover, progression biopsies are rarely acquired from mBC patients, making posttreatment tumor analysis difficult. Given the value of understanding prognostic and predictive biomarkers, this paradigm is changing. Importantly, biomarker analysis of pre-and posttreatment specimens from several neoadjuvant trials, now in progress or completed, will enable us to assess the clinical implications of the preclinical markers identified for T-DM1 resistance.

Disclosure of Potential Conflicts of Interest

M.X. Sliwkowski has an ownership interest (including patents) in, and is a consultant/advisory board member for, Genentech, Inc. No potential conflicts of interest were disclosed by the other authors.

Authors' Contributions

Conception and design: G. Li, M.X. Sliwkowski, G.D.L. Phillips
Development of methodology: G. Li, J. Guo, B.-Q. Shen
Acquisition of data (provided animals, acquired and managed patients, provided facilities, etc.): G. Li, J. Guo, D.B. Yadav, L.M. Crocker, J.A. Lacap
Analysis and interpretation of data (e.g., statistical analysis, biostatistics, computational analysis): G. Li, J. Guo, B.-Q. Shen, D.B. Yadav, G.D.L. Phillips
Writing, review, and/or revision of the manuscript: G. Li, J. Guo, B.-Q. Shen, D.B. Yadav, M.X. Sliwkowski, G.D.L. Phillips
Administrative, technical, or material support (i.e., reporting or organizing data, constructing databases): G. Li, L.M. Crocker
Study supervision: G. Li, M.X. Sliwkowski

Acknowledgments

We thank Suzie J. Scales for running HER2 immunofluorescence assays and Suchit Jhunjhunwala for microarray data analysis.

The costs of publication of this article were defrayed in part by the payment of page charges. This article must therefore be hereby marked *advertisement* in accordance with 18 U.S.C. Section 1734 solely to indicate this fact.

Received March 31, 2017; revised August 3, 2017; accepted April 12, 2018; published first April 25, 2018.

References

1. Yarden Y, Sliwkowski MX. Untangling the ErbB signalling network. Nat Rev Mol Cell Biol 2001;2:127–37.
2. Slamon DJ, Clark GM, Wong SG, Levin WJ, Ullrich A, McGuire WL. Human breast cancer: correlation of relapse and survival with amplification of the HER-2/neu oncogene. Science 1987;235:177–82.
3. Cho HS, Mason K, Ramyar KX, Stanley AM, Gabelli SB, Denney DW, et al. Structure of the extracellular region of HER2 alone and in complex with the Herceptin Fab. Nature 2003;421:756–60.
4. Slamon DJ, Leyland-Jones B, Shak S, Fuchs H, Paton V, Bajamonde A, et al. Use of chemotherapy plus a monoclonal antibody against HER2 for metastatic breast cancer that overexpresses HER2. N Engl J Med 2001;344:783–92.
5. Smith I, Procter M, Gelber RD, Guillaume S, Feyereislova A, Dowsett M, et al. 2-year follow-up of trastuzumab after adjuvant chemotherapy in HER2-positive breast cancer: a randomised controlled trial. Lancet 2007;369:29–36.
6. Nagata Y, Lan KH, Zhou X, Tan M, Esteva FJ, Sahin AA, et al. PTEN activation contributes to tumor inhibition by trastuzumab, and loss of PTEN predicts trastuzumab resistance in patients. Cancer Cell 2004;6:117–27.
7. Junttila TT, Akita RW, Parson K, Fields C, Lewis Phillips GD, Friedman LS, et al. Ligand-independent HER2/HER3/PI3K complex is disrupted by trastuzumab and is effectively inhibited by the PI3K inhibitor GDC-0941. Cancer Cell 2009;15:429–40.
8. Molina MA, Codony-Servat J, Albanell J, Rojo F, Arribas J, Baselga J. Trastuzumab (herceptin), a humanized anti-Her2 receptor monoclonal antibody, inhibits basal and activated Her2 ectodomain cleavage in breast cancer cells. Cancer Res 2001;61:4744–9.

9. Sliwkowski MX, Lofgren JA, Lewis GD, Hotaling TE, Fendly BM, Fox JA. Nonclinical studies addressing the mechanism of action of trastuzumab (Herceptin). Sem Oncol 1999;26:60–70.
10. Izumi Y, Xu L, di Tomaso E, Fukumura D, Jain RK. Tumour biology: herceptin acts as an anti-angiogenic cocktail. Nature 2002;416: 279–80.
11. Pohlmann PR, Mayer IA, Mernaugh R. Resistance to trastuzumab in breast cancer. Clin Cancer Res 2009;15:7479–91.
12. Molina MA, Saez R, Ramsey EE, Garcia-Barchino MJ, Rojo F, Evans AJ, et al. NH(2)-terminal truncated HER-2 protein but not full-length receptor is associated with nodal metastasis in human breast cancer. Clin Cancer Res 2002;8:347–53.
13. Lu Y, Zi X, Zhao Y, Mascarenhas D, Pollak M. Insulin-like growth factor-I receptor signaling and resistance to trastuzumab (Herceptin). J Natl Cancer Inst 2001;93:1852–7.
14. Lewis Phillips GD, Li G, Dugger DL, Crocker LM, Parsons KL, Mai E, et al. Targeting HER2-positive breast cancer with trastuzumab-DM1, an antibody-cytotoxic drug conjugate. Cancer Res 2008;68: 9280–90.
15. Junttila TT, Li G, Parsons K, Phillips GL, Sliwkowski MX. Trastuzumab-DM1 (T-DM1) retains all the mechanisms of action of trastuzumab and efficiently inhibits growth of lapatinib insensitive breast cancer. Breast Cancer Res Treat 2011;128:347–56.
16. Verma S, Miles D, Gianni L, Krop IE, Welslau M, Baslega J, et al. Trastuzumab emtansine for HER2-positive advanced breast cancer. N Engl J Med 2012;367:1783–91.
17. Kurebayashi J, Otsuki T, Tang CK, Kurosumi M, Yamamoto S, Tanaka K, et al. Isolation and characterization of a new human breast cancer cell line, KPL-4, expressing the Erb B family receptors and interleukin-6. British J Cancer 1999;79:707–17.
18. Shang Y, Mao Y, Batson J, Scales SJ, Phillips G, Lackner MR, et al. Anti-xenograft tumor activity of a humanized anti-insulin-like growth factor-I receptor monoclonal antibody is associated with decreased AKT activation and glucose uptake. Mol Cancer Ther 2008;7:2599–608.
19. Folkes AJ, Ahmadi K, Alderton WK, Alix S, Baker SJ, Box G, et al. The identification of 2-(1H-indazol-4-yl)-6-(4-methanesulfonyl-piperazin-1-ylmethyl)-4-morpholin-4-yl-thienol[3,2-d]pyrimidine (GDC-0941) as a potent, selective, orally bioavailable inhibitor of class I PI3 kinase for the treatment of cancer. J Med Chem 2008;51:5522–32.
20. Dale IL, Tuffley W, Callaghan R, Holmes JA, Martin K, Luscombe M, et al. Reversal of P-glycoprotein-mediated multidrug resistance by XR9051, a novel diketopiperazine derivative. British J Cancer 1998;78: 885–92.
21. Allen JD, van Loevezjin A, Lakhai JM, van der Valk M, van Tellingen O, Reid G, et al. Potent and specific inhibition of the breast cancer resistance protein multidrug transporter in vitro and in mouse intestine by a novel analogue of fumitremorgin C. Mol Cancer Ther 2002;1:417–25.
22. Christensen JG, Schreck R, Burrows J, Kuruganti P, Chan E, Le P, et al. A selective small molecule inhibitor of c-met kinase inhibits c-met-dependent phenotypes in vitro and exhibits cytoreductive antitumor activity in vivo. Cancer Res 2003;63:7345–55.
23. Hatse S, Princen K, Bridger G, De Clercq E, Schols D. Chemokine receptor inhibition by AMD3100 is strictly confined to CXCR4. FEBS Lett 2002; 527:255–62.
24. Oroudjev E, Lopus M, Wilson L, Audette C, Provenzano C, Erickson H, et al. Maytansinoid-antibody conjugates induce mitotic arrest by suppressing microtubule dynamic instability. Mol Cancer Ther 2010;9: 2700–13.
25. Hoeflich KP, Gray DC, Eby MT, Tien JY, Wong L, Bower J, et al. Oncogenic BRAF is required for tumor growth and maintenance in melanoma models. Cancer Res 2006;66:999–1006.
26. Lewis Phillips GD, Fields CT, Li G, Dowbenko D, Schaefer G, Miller K, et al. Dual targeting of HER2-positive cancer with trastuzumab emtansine and pertuzumab: critical role for neuregulin blockade in antitumor response to combination therapy. Clinical Cancer Res 2014;20:456–68.
27. Chou TC. Theoretical basis, experimental design, and computerized simulation of synergism and antagonism in drug combination studies. Pharmacol Rev 2006;58:621–81.
28. Rios-Luci C, Garcia-Alonso S, Diaz-Rodriguez E, Nadal-Serrano M, Arribas J, Ocana A, et al. Resistance to the antibody-drug conjugate T-DM1 is based in a reduction in lysosomal proteolytic activity. Cancer Res 2017;77: 4639–51.
29. Pellegrino R, Kavakli IH, Goel N, Cardinale CJ, Dinges DF, Kuna ST, et al. A novel BHLHE41 variant is associated with short sleep and resistance to sleep deprivation in humans. Sleep 2014;37: 1327–36.
30. Kreslavsky T, Vilagos B, Tagoh H, Poliakova DK, Schwickert TA, Wohner M, et al. Essential role for the transcription factor Bhlhe41 in regulating the development, self-renewal and BCR repertoire of B-1a cells. Nat Immunol 2017;18:442–55.
31. Montagner M, Enzo E, Forcato M, Zanconato F, Parenti A, Rampazzo E, Basso G, et al. SHARP1 suppresses breast cancer metastasis by promoting degradation of hypoxia-inducible factors. Nature 2012;487: 380–4.
32. Baselga J, Lewis Phillips GD, Verma S, Ro J, Huober J, Guardino AE, et al. Relationship between tumor biomarkers and efficacy in EMILIA, a phase III study of trastuzumab emtansine in HER2-positive metastatic breast cancer. Clin Cancer Res 2016;22:3755–63.
33. Erickson HK, Lewis Phillips GD, Leipold DD, Provenzano CA, Mai E, Johnson HA, et al. The effect of different linkers on target cell catabolism and pharmacokinetics/pharmacodynamics of trastuzumab maytansinoid conjugates. Mol Cancer Ther 2012;11:1133–42.
34. Harbinski F, Craig VJ, Sanghavi S, Jeffery D, Liu L, Sheppard KA, et al. Rescue screens with secreted proteins reveal compensatory potential of receptor tyrosine kinases in driving cancer growth. Cancer Disc 2012;2:948–59.
35. Nahta R, Yu D, Hung MC, Hortobagyi GN, Esteva FJ. Mechanisms of disease: understanding resistance to HER2-targeted therapy in human breast cancer. Nat Clin Practice Oncol 2006;3:269–80.
36. Shattuck DL, Miller JK, Carraway KL 3rd, Sweeney C. Met receptor contributes to trastuzumab resistance of Her2-overexpressing breast cancer cells. Cancer Res 2008;68:1471–7.
37. Wilson TR, Fridlyand J, Yan Y, Penuel E, Burton L, Chan E, Peng J, et al. Widespread potential for growth-factor-driven resistance to anticancer kinase inhibitors. Nature 2012;487:505–10.
38. Hegde GV, de la Cruz CC, Chiu C, Alag N, Schaefer G, Crocker L, et al. Blocking NRG1 and other ligand-mediated HER4 signaling enhances the magnitude and duration of the chemotherapeutic response of non-small cell lung cancer. Science Transl Med 2013;5:171ra18.
39. Berns K, Horlings HM, Hennessy BT, Madiredjo M, Hijmans EM, Beelen K, et al. A functional genetic approach identifies the PI3K pathway as a major determinant of trastuzumab resistance in breast cancer. Cancer Cell 2007;12:395–402.
40. Hamel S, Bouchard A, Ferrario C, Hassan S, Aguilar-Mahecha A, Buchanan M, et al. Both t-Darpp and DARPP-32 can cause resistance to trastuzumab in breast cancer cells and are frequently expressed in primary breast cancers. Breast Cancer Res Treat 2010;120:47–57.
41. Szakacs G, Paterson JK, Ludwig JA, Booth-Genthe C, Gottesman MM. Targeting multidrug resistance in cancer. Nature Rev Drug Disc 2006; 5:219–34.
42. El-Gebali S, Bentz S, Hediger MA, Anderle P. Solute carriers (SLCs) in cancer. Mol Aspects Med 2013;34:719–34.
43. Hamblett KJ, Jacob AP, Gurgel JL, Tometsko ME, Rock BM, Patel SK, et al. SLC46A3 is required to transport catabolites of noncleavable antibody maytansine conjugates from the lysosome to the cytoplasm. Cancer Res 2015;75:5329–40.
44. Loganzo F, Tan X, Sung M, Jin G, Myers JS, Melamud E, et al. Tumor cells chronically treated with trastuzumab-maytansinoid antibody-drug conjugate develop varied resistance mechanisms but respond to alternate treatments. Mol Cancer Ther 2015;14:952–63.
45. Yu SF, Zheng B, Go M, Lau J, Spencer S, Raab H, et al. A novel anti-CD22 anthracycline-based antibody-drug conjugate (ADC) that overcomes resistance to auristatin-based ADCs. Clin Cancer Res 2015;21: 3298–306.
46. Chen R, Hou J, Newman E, Kim Y, Donohue C, Liu X, et al. CD30 downregulation, MMAE resistance, and MDR1 upregulation are all associated with resistance to brentuximab vedotin. Molr Cancer Ther 2015;14:1376–84.
47. Nagy P, Friedlander E, Tanner M, Kapanen AI, Carraway KL, Isola J, et al. Decreased accessibility and lack of activation of ErbB2 in JIMT-1, a

Herceptin-resistant, MUC4-expressing breast cancer cell line. Cancer Res 2005;65:473–82.
48. Pandolfi PP. Breast cancer–loss of PTEN predicts resistance to treatment. N Engl J Med 2004;351:2337–8.
49. Cheng H, Ballman K, Vassilakopoulou M, Dueck AC, Reinholz MM, Tenner K, et al. EGFR expression is associated with decreased benefit from trastuzumab in the NCCTG N9831 (Alliance) trial. Br J Cancer 2014;111:1065–71.
50. Sabbaghi MA, Gil-Gomez G, Guardia C, Servitja S, Arpi O, Garcia-Alonso S, et al. Defective cyclin B1 in trastuzumab emtansine (T-DM1) acquired resistance in HER2-positive breast cancer. Clin Cancer Res 2017;23:7006–19.